International Science and Technology Journal
المجلة الدولية للعلوم والتقنية
Volume 36 العدد
Part 2 المجلد
ISTJ

http://www.doi.org/10.62341/jfaa2057

Received	2025/04/29	تم استلام الورقة العلمية في
Accepted	2025/05/25	تم قبول الورقة العلمية في
Published	2025/05/27	تم نشر الورقة العلمية في

The Effectiveness of the Metallic Reinforcement Phase on the Solidification Process of Medium-Carbon Steel Castings

Jamal Ibrahim Musbah[1], Fareg S. Ali[1], Ali Al-Taib Al-Siebaie[2], Aimen M. Albakoush[1].

[1]Mechanical Engineering Department, College of Science and Technology - Bani Walid - Libya
[2]Mechanical Engineering Department, Higher Institute of Engineering Technology- Sabha - Libya
jamal.musbah@ctsbw.edu.ly

Abstract

This study investigates the effect of the metallic reinforcement phase on the properties of castings made from medium-carbon steel using the Lost Foam Process. Numerical simulations were conducted using ESI-ProCast v2121.5 software to analyze the influence of sample sizes and reinforcement ratios on cooling rates and crystalline properties. The study included samples with dimensions of 10Ø×200 mm and 50Ø×200 mm, with reinforcement ratios of 0% and 50%.

The results demonstrated that the introduction of reinforcement phase particles significantly enhances cooling rates and improves the crystalline structure, thereby enhancing the mechanical properties of the castings. Statistical analyses, including variance analysis, revealed that the optimal range of reinforcement ratios lies between 12% and 33%. This range offers a balance between solidification speed and the reduction of structural voids while maintaining the fluidity of the molten metal. Ratios exceeding 33% negatively impacted fluidity, hindering the casting process.

This study highlights the potential of innovative mold designs that strategically incorporate the reinforcement phase to optimize cooling rates while reducing harmful environmental emissions. The findings contribute to advancing sustainable casting practices by improving product quality and minimizing environmental impacts, providing a solid foundation for future industrial applications.

http://www.doi.org/10.62341/jfaa2057

Keywords: Lost Foam Process, Casting, Polystyrene Foam, Metallic Reinforcement Phase, Metal Matrix Composites, Cooling Rate.

فعالية الطور المعدني المقوّي على عملية التصلب في سبائك الصلب متوسطة الكربون

جمال إبراهيم مصباح[1]، فرج سعيد علي[1]، علي التايب السبيعي[2]، ايمن محمد البكوش[1]

[1] قسم الهندسة الميكانيكية، كلية العلوم والتقنية – بني وليد – ليبيا

[2] قسم الهندسة الميكانيكية، المعهد العالي للتقنية الهندسية – سبها – ليبيا

jamal.musbah@ctsbw.edu.ly

الملخص

تستكشف هذه الدراسة تأثير طور التسليح المعدني على خصائص المسبوكات المصنوعة من الصلب متوسط الكربون باستخدام تقنية الصب بالنماذج الغازية، تم إجراء محاكاة رقمية باستخدام برنامج (ESI–ProCast v2121.5) لتحليل تأثير حجم العينات ونسب التعزيز على معدلات التبريد والخصائص البلورية. تضمنت الدراسة عينات بأبعاد 10×200 ملم و50×200 ملم مع نسب تعزيز حجمي 0% و50 % .أظهرت النتائج أن إدخال جسيمات طور التسليح يحسن بشكل كبير من معدل التبريد ويُحسِّن البنية البلورية، مما يعزز الخصائص الميكانيكية للمسبوكات. أظهرت التحليلات الإحصائية، بما في ذلك حساب التباين، أن النطاق الأمثل لنسب التعزيز يتراوح بين 12% و33%، حيث يوفر هذا النطاق توازنًا بين سرعة التصلب وتقليل الفراغات الهيكلية مع الحفاظ على سيولة المعدن المصهور. وأظهرت النسب التي تزيد عن 33% تأثيرًا سلبيًا على خاصية السيولة، مما يعيق عملية الصب.

تسلط هذه الدراسة الضوء على فعالية التصميمات المبتكرة لقوالب الصب التي تدمج طور التعزيز بطريقة استراتيجية لتحسين معدلات التبريد مع تقليل الانبعاثات البيئية الضارة. تسهم النتائج في تعزيز ممارسات السباكة المستدامة من خلال تحسين جودة المنتج وتقليل التأثيرات البيئية، مما يوفر أساسًا متينًا للتطبيقات الصناعية المستقبلية.

الكلمات المفتاحية: الصب باستخدام النماذج الغازية، المسبوكات الضخمة، نموذج رغوة البولسترين، طور التعزيز المعدني، سبائك البنى البلورية المعززة، معدل التبريد للسبيكة.

http://www.doi.org/10.62341/jfaa2057

Introduction

As modern industrial production evolves, the demand for environmentally friendly and highly efficient technologies has become a strategic imperative across multiple sectors of the national economy. Research efforts are directed towards finding innovative solutions to achieve sustainability and reduce environmentally harmful byproducts, while focusing on the safe rationalization of natural resource consumption.

Lost Foam Process (LFP) casting technologies are among the most prominent of these solutions, as they eliminate the need for many traditional, cost-intensive, and energy-demanding processes, thus contributing to improved efficiency and reduced negative environmental impacts [1].

Studies indicate that incorporating a Metallic Reinforcement Phase (MRP) into the polystyrene molding process can enhance the mechanical properties of the produced materials, either by mixing it with the polystyrene material or distributing it within the mold [2, 3].

Metal Matrix Composites (MMC) containing various reinforcing phases have demonstrated attractive advantages such as high specific strength, stiffness, and wear resistance, making them preferred materials for multiple applications including engineering, aerospace, electronics, and automotive industries [4-7].

Many recent studies have focused on aluminum as a primary matrix material (MMC) due to its lightweight and excellent properties. For example, a study by Huang et al. (2018) showed that reinforcing aluminum with titanium particles led to a 55% improvement in tensile strength due to grain refinement and boundary strengthening [8]. A study by Rashad et al. (2015) confirmed the improvement in the mechanical properties of magnesium by incorporating titanium particles into the matrix [9].

In contrast, iron alloys and cast iron have not received the same level of attention despite their significant importance in heavy-duty applications. Some studies have explored using iron particles to reinforce aluminum, noting significant improvements in hardness and tensile strength [10]. A study by Musbah J. et al. (2021) also indicated the effect of steel particles on the reinforcement of cast iron, where uniform carbon distribution led to improved mechanical properties of the alloy [11].

Additionally, a study by Shalevska (2019) analyzed the impact of the reinforcement phase on controlling localized overheating and

http://www.doi.org/10.62341/jfaa2057

cooling rates within the mold, enabling the creation of locally reinforced areas within the castings [12].

These research gaps highlight the need to explore the possibilities of producing large castings using lost foam casting with polystyrene patterns, while introducing reinforcing particles to enhance the crystalline structure and reduce harmful emissions [13-18].

The current study aims to improve the quality of massive castings and enhance their mechanical properties by accelerating the cooling process using reinforcement particles, with a focus on reducing emissions resulting from the use of expanded polystyrene patterns.

Literature Review

The integration of metallic reinforcement phases (MRPs) into casting processes—especially when used in conjunction with the Lost Foam Process (LFP)—has been increasingly explored to enhance the mechanical performance, solidification behavior, and environmental sustainability of metal matrix composites (MMCs).

Abraham et al. (2019) examined the effects of vanadium particle reinforcement on the mechanical properties of aluminum alloy AA6063 composites [19]. Their results indicated a significant improvement in hardness and tensile strength, attributed to refined grain structure and effective load transfer from the matrix to the reinforcement. This finding supports the premise that MRPs serve as effective thermal conductors and nucleation sites during solidification.

Alaneme et al. (2018) studied Al-Mg-Si alloys reinforced with steel particles and found that MRPs significantly enhanced mechanical resistance, particularly under compressive and wear conditions [10]. These results reinforce the role of steel particles in improving core mechanical properties, which aligns with the use of steel particles in the current study for medium-carbon steel castings.

Musbah J. et al. (2021) explored how reinforcing mold patterns with metallic inserts impacted casting structure during pouring. Their findings demonstrated that such reinforcements led to more uniform cooling and minimized porosity in the final product [11]. This confirms the simulation results in the present study, where the integration of MRPs increased the cooling rate and reduced internal voids. Similarly, Metalcast S.A. de C.V. (2013) utilized the ESI ProCAST software to identify and mitigate porosity defects in valve body castings. By iteratively adjusting simulation parameters and refining mold designs based on the results, the company

http://www.doi.org/10.62341/jfaa2057

successfully reduced casting rejection rates from 25% to 3%, demonstrating the effectiveness of ProCAST in predictive defect analysis and process optimization [20].

Shalevska (2019) also investigated heat transfer processes within reinforced molds and concluded that MRPs significantly reduce thermal resistance, enabling faster heat dissipation [12]. These results are consistent with the current simulation findings, where reinforced samples showed up to a threefold reduction in solidification time compared to unreinforced ones.

Doroshenko and Chichkan (2008) focused on gas regime control in LFP molds for large castings. Their insights showed that managing gas pressure and composition during polystyrene combustion can enhance mold-filling efficiency, especially when reinforcement is involved [13]. These findings align with the conclusion of this study regarding the optimal ratio between reinforcement content and mold filling efficiency.

Mamyshev et al. (2010) systematically analyzed the crystallization of castings with different reinforcement scenarios. They showed that localized reinforcement helps in tailoring the grain structure for specific mechanical properties [15]. This supports the current study's suggestion that optimal reinforcement (12–33%) not only speeds up cooling but also enhances the crystalline arrangement.

Ryabicheva et al. (2010) investigated porous metallic structures and their thermal response under deformation [16]. The study indicated that porosity and reinforcement distribution can affect heat conduction and stress dissipation during solidification. These parameters are vital in explaining why reinforcement beyond 33% reduced fluidity and led to premature solidification in this study.

Lastly, Shalevska et al. (2015) highlighted the environmental impact of casting emissions and how integrating MRPs into LFP molds significantly reduces polystyrene combustion residues [17]. The present study supports this observation, stating that optimized reinforcement ratios lower the temperature and volume of combustion gases, thus reducing environmental emissions.

Methodology

The methodology of this study involves conducting simulations using ESI ProCAST v2021.5, an advanced simulation tool based on the finite element method. The software facilitates virtual modeling of various casting processes, such as sand casting, die casting, and investment casting, while enabling the prediction of common

http://www.doi.org/10.62341/jfaa2057

casting defects like porosity, shrinkage, and thermal stresses [21]. In this research, ProCAST is utilized to assess the thermal behavior of both reinforced and unreinforced alloys during heating and cooling stages, along with performing associated calculations, following the approach outlined below:

1. Specimen Size Selection: Simulations were performed on two specimen sizes: the first with dimensions of 10 mm in diameter and 200 mm in length, and the second with dimensions of 50 mm in diameter and 200 mm in length. The specimens were made of Carbon Steel Grade 45, with the composition as shown in Table 1.

Table 1. Chemical Composition of the Carbon Steel 45 Alloy Used as the MMC Matrix

Element	Iron (Fe)	Carbon (C)	Silicon (Si)	Manganese (Mn)	Phosphorus (P)	Sulfur (S)
Percentage (%)	98.89	0.45	0.10	0.50	0.04	0.02

2. **Reinforcement Ratios for Specimens:**

The sample set was classified into two types based on the reinforcement level:

A. **Unreinforced specimens:** For both sizes (10 mm diameter x 200 mm and 50 mm diameter x 200 mm).

B. **Specimens with Reinforcement Particles (MRP):** At a ratio of 50% by volume for both sizes.

The Reinforcement Particles (MRP) were made of Carbon Steel Grade 20, with the composition shown in Table 2:

Table 2. Chemical Composition of the Carbon Steel 20 Alloy Used as Reinforcement Particles (MRP)

Element	Iron (Fe)	Carbon (C)	Silicon (Si)	Manganese (Mn)	Phosphorus (P)	Sulfur (S)
Percentage (%)	98.04	0.22	0.45	1.25	0.03	0.01

3. **Casting Mold:** The simulation study was performed for the casting mold using expanded polystyrene (EPS) patterns, according to the design prepared in Figure 1-a. The alternative mold reinforcement design in Figure 1-b was also designed for casting cases that do not involve polystyrene patterns and are used for other casting methods, such as sand casting.

http://www.doi.org/10.62341/jfaa2057

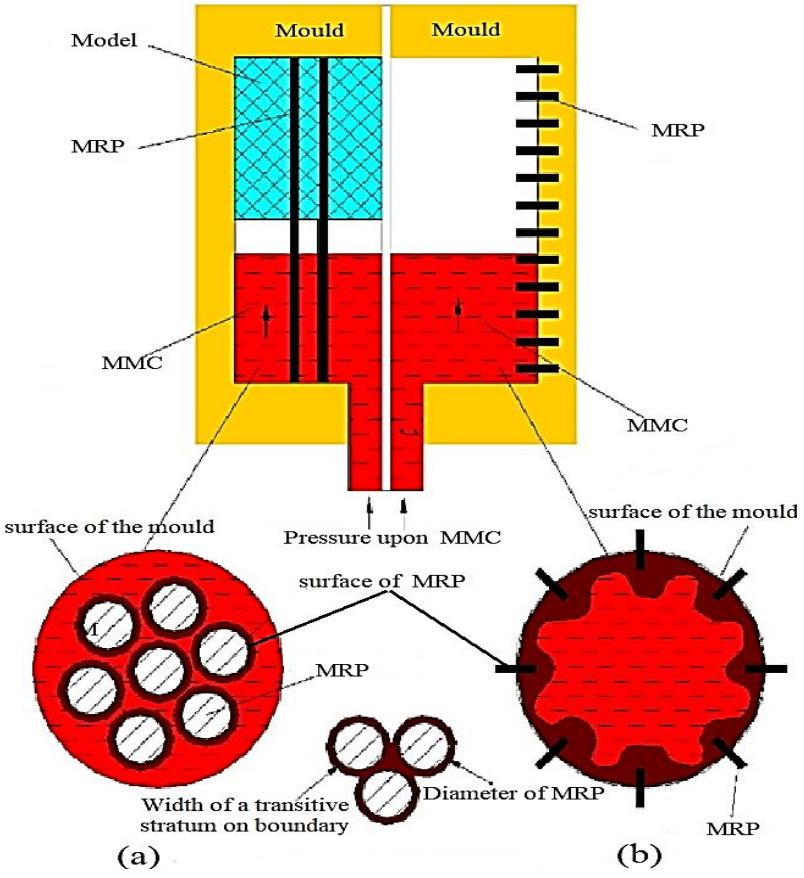

Figure 1-a. Design of RMP structures within polystyrene foam molds.
b. Configuration of RMP distribution in molds without polystyrene foam [25].

It is also possible to reduce the amount of polystyrene used by using intermediate designs between the two designs, leaving a layer of polystyrene on the areas that provide product details, which in turn will give the desired final finish and precision, and on the areas that serve as filler for the surfaces. This type of design is considered a good option to reduce the level of harmful emissions resulting from the combustion of polystyrene.

4. Mathematical and Statistical Calculations:

In addition to the casting simulation, several calculations were performed, including:

http://www.doi.org/10.62341/jfaa2057

4.1. Effect of Alloy Elements on the Liquidus and Solidus Curves: As is known, the alloy is carbon steel grade 45, meaning that the carbon content is around 0.45%, as shown in Table 1. Consequently, the liquidus line is at 1490°C and the solidus line is at 1475°C, according to the iron-carbon phase diagram. However, these limits change depending on the variation in the percentages of alloying elements [22,23]. Table 3 shows the effect of 1% of added elements on the liquidus and solidus lines, according to the chemical composition of grade 45 steel.

Table 3. Effect of Casting Elements on the Temperatures of Liquidus and Solidus Curves

Element	Change in Liquidus Temperature ($\Delta T liquidus$) (°C per 1%)	Change in Solidus Temperature ($\Delta T solidus$) (°C per 1%)
Silicon (Si)	+10	+15
Manganese (Mn)	-2	-5
Phosphorus (P)	-30	-50
Sulfur (S)	-6	-8

The temperatures for the liquidus and solidus phases are calculated according to the following mathematical equations [24]:

$$T_{liquidus} = T_{base} + \sum_{i=1}^{n} \left(x_i . \Delta T_{liquidus,i} \right) \quad (1)$$

$$T_{solidus} = T_{base} + \sum_{i=1}^{n} \left(x_i . \Delta T_{solidus,i} \right) \quad (2)$$

Where:

- $T_{liquidus}$: Final temperature of the liquidus line.
- $T_{solidus}$: Final temperature of the solidus line.
- T_{base}: Base temperature of the liquidus line (Equation 1) and the solidus line (Equation 2) according to the iron-carbon phase diagram.
- x_i: Percentage of the element in the alloy.
- $\Delta T_{liquidus,i}$: The change in the liquidus line temperature caused by 1% of element (i).
- $\Delta T_{solidus,i}$: The change in the solidus line temperature caused by 1% of element (i).

http://www.doi.org/10.62341/jfaa2057

4.2. Linear Interpolation Calculation: The following linear interpolation equation was used:

$$y = y_1 + \frac{(x - x_1).(y_2 - y_1)}{(x_2 - x_1)} \quad (3)$$

Where:

- y: The temperature at a specific time (x).
- x: The time value at which the temperature (y) is to be calculated.
- (x_1, y_1): The first known data point, representing a time before (x) and its corresponding temperature (y_1).
- (x_2, y_2): The second known data point, representing a time after (x) and its corresponding temperature (y_2).

This methodology is employed to determine accurate intermediate points on the solidification curve. This curve represents the relationship between liquid and solid phases. The objective is to facilitate the calculation of temperature variation between different levels within a casting (surface, quarter-depth, and center). Additionally, Equation (4) is used to perform interpolation between an unreinforced sample and a sample reinforced with 50% volume fraction, using a sequential series of reinforcement percentages (10%, 20%, 25%, 30%, 35%, 40%). This approach aims to identify the optimal reinforcement percentage that minimizes thermal deviation, while also achieving a balanced cooling rate that considers both the speed of cooling and insufficient heat dissipation within the casting.

$$T_{i\%} = T_{0\%} + \frac{i\%}{50}.(T_{50\%} - T_{0\%}) \quad (4)$$

Where:

$T_{i\%}$:The temperature corresponding to the specified reinforcement percentage $(i\%)$.

$T_{0\%}$:The temperature of the sample without reinforcement, equivalent to the time-temperature for reinforcement. (50%).

$T_{50\%}$: The temperature of the sample with 50%reinforcement, equivalent to the time-temperature for reinforcement (0%).

4.3. The standard deviation calculation: To evaluate the variation between levels and different reinforcement ratios, the standard deviation is calculated using the following equation:

(5)

http://www.doi.org/10.62341/jfaa2057

$$\sigma_{\%} = \sqrt{\frac{1}{n}\sum_{i=1}^{n}(\mu - x_i)^2}$$

Where:
$\sigma_{\%}$:The standard deviation of the different reinforcement ratios.
n :The number of values in the dataset.
x_i :The individual data values.
μ :The arithmetic mean of the samples with different reinforcement ratios.

$$s_L = \frac{1}{1-n}\sum_{i=1}^{n}(x_i - \bar{x})^2 \quad (6)$$

Where:
s_L :The standard deviation of the sample levels (surface-quarter-center).
$\bar{x}$:The arithmetic mean of the levels within the sample.

Discussion and Results

The introduction of a reinforcement phase into polystyrene foam models or directly into the mold cavity enables the creation of new cast structures with a range of functional properties that were not previously inherent in traditional casting alloys.

A Sample with a Diameter of 10 mm without Reinforcement Phase:

It was determined that the alloy reaches the liquidus temperature (T_L) of 1475°C for the matrix alloy at the "metal-mold" contact surface after 0.5 seconds (Figure 2). The solidus temperature (T_s) is reached after 10.8 seconds. Meanwhile, at the point corresponding to ¼ of the sample diameter, the alloy reaches the liquidus temperature T_L after 2.1 seconds (Figure 2) and the solidus temperature T_s after 11.8 seconds. At the center of the sample, the alloy reaches the liquidus temperature T_L after 2.2 seconds (Figure 2) and the solidus temperature T_s after 12.6 seconds. The liquid phase then disappears in all sections of the casting, as shown in Figure 3.

http://www.doi.org/10.62341/jfaa2057

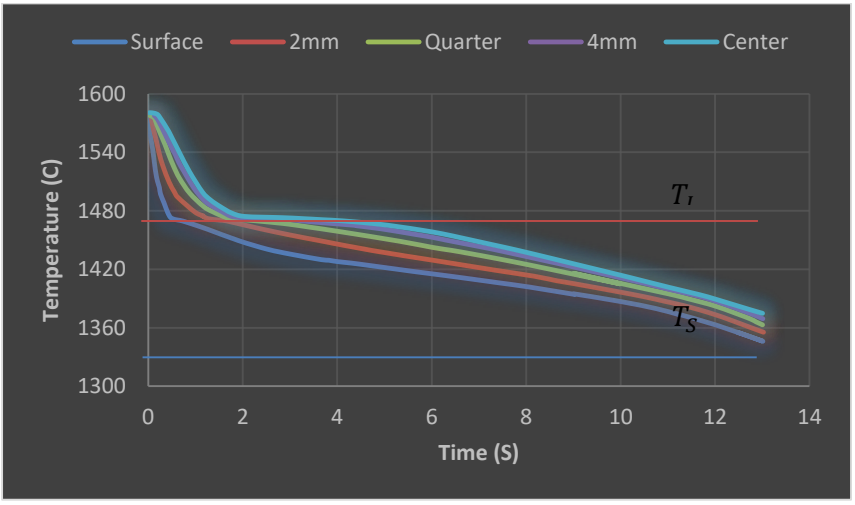

Figure 2**.** Solidification and cooling kinematics of the casting for a sample (Ø10×200 mm) made of 45 steel in the mold cavity.

Figure 3 illustrates the simulation of the mixed phase (liquid and solid phases) over time, starting from the liquidus line, representing 100% liquid, to the solidus line at 0% liquid for the same sample.

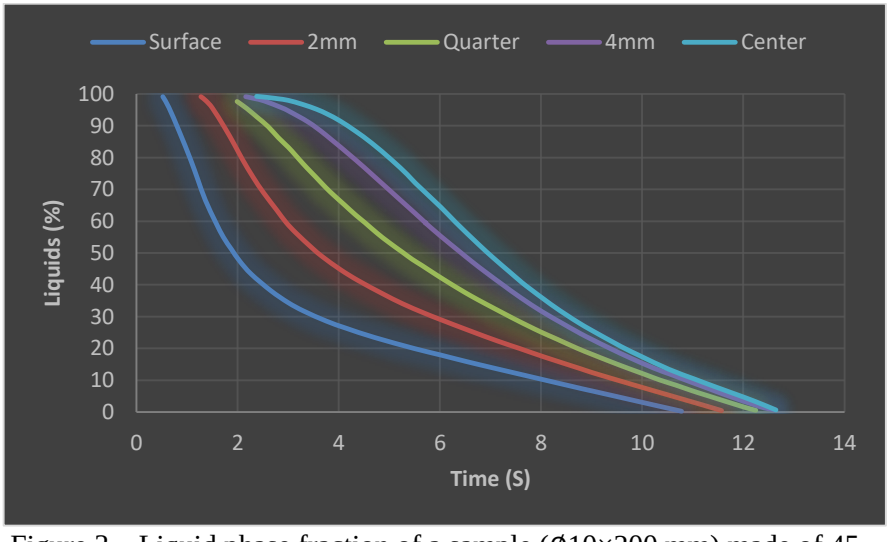

Figure 3 – Liquid phase fraction of a sample (Ø10×200 mm) made of 45 steel during the cooling time.

A Sample with a Diameter of 10 mm and 50% Reinforcement:
During the solidification of a 10 mm diameter sample in a reinforced mold occupying half of its cross-sectional area, it was observed that the alloy reached the liquidus temperature (T_l) after 0.4 seconds at

http://www.doi.org/10.62341/jfaa2057

the metal-mold contact surface, as shown in Figure 4. The solidus temperature (T_s) — corresponding to 0% liquid fraction — was reached after 2.2 seconds, as depicted in Figure 5. During this interval, at a point located at ¼ of the sample's diameter and at the metal-MRP boundary, the alloy reached the liquidus temperature (T_l) after 0.2 seconds and the solidus temperature (T_s) after 2.8 seconds. At this stage, the liquid phase disappeared completely across all sections of the casting (Figure 5).

It is noteworthy that under these conditions, the reinforcement phase (MRP) near the center of the alloy experienced a rapid temperature rise, reaching 980°C within 0.5 seconds. This phenomenon, referred to as thermal shock, caused a gradient in temperature levels. Subsequently, the reinforcement phase cooled at a rate of 6–8°C/second (Figures 4–5).

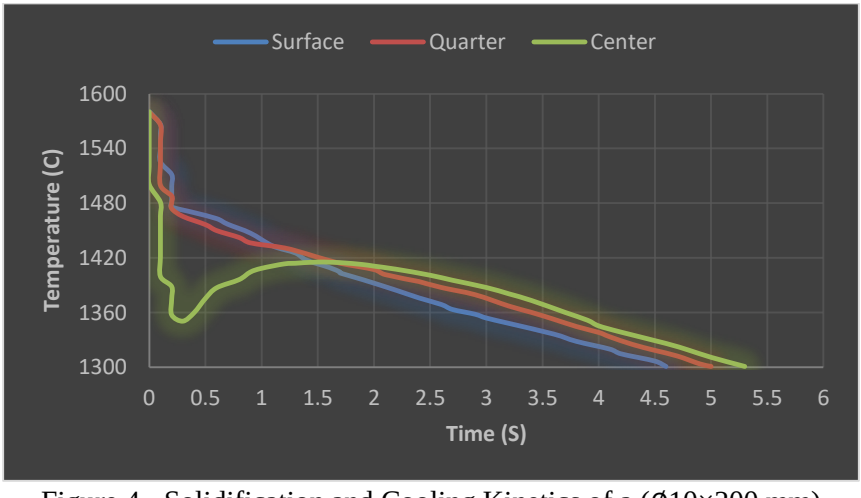

Figure 4 - Solidification and Cooling Kinetics of a (Ø10×200 mm) Sample of 45 Steel Reinforced with 50%.

http://www.doi.org/10.62341/jfaa2057

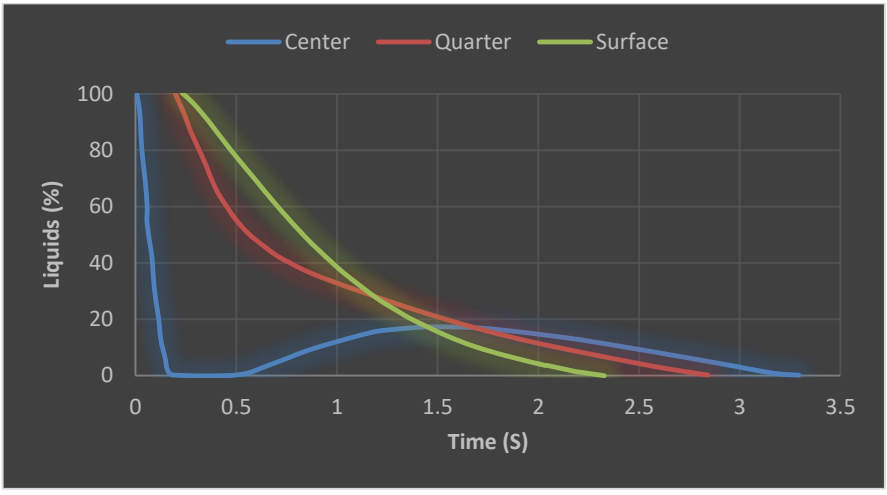

Figure 5 – Liquid Phase Fractions of a 50% Reinforced Sample with Dimensions (Ø10×200 mm) During Cooling Time.

A Sample with a Diameter of 50 mm Without the Reinforcement Phase (MRP):

In the computational simulation of the solidification of a 50 mm diameter sample made of medium-carbon steel (grade 45) within a hollow mold, it was determined that the alloy at the metal-mold contact surface reached the liquidus temperature (T_l) after 9.8 seconds, as illustrated in Figure 6. The solidus temperature (T_s), corresponding to 0% liquid fraction, was reached after 182.0 seconds, representing the solidification boundary in the liquid-solid fraction curve shown in Figure 7.

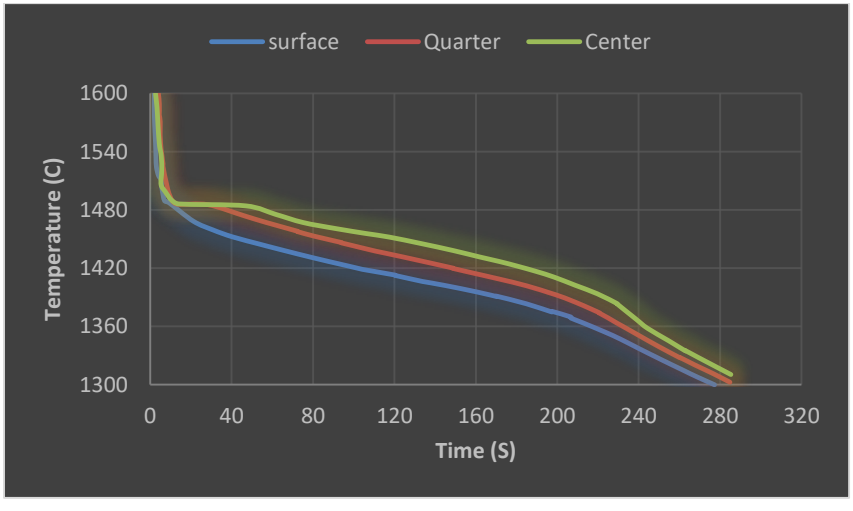

http://www.doi.org/10.62341/jfaa2057

Figure 6 – Solidification and Cooling Kinetics of the Casting (Diameter 50 × 200 mm) Made of 45 Steel Without Reinforcement.

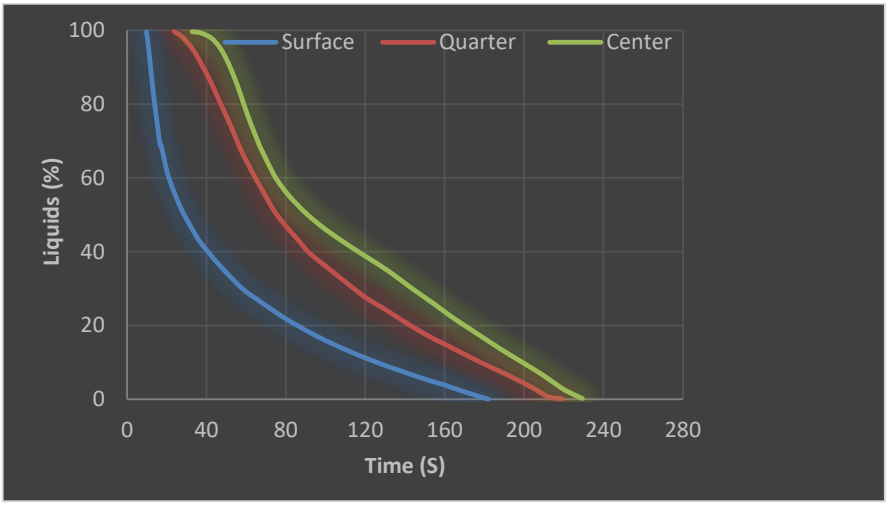

Figure 7 – Liquid Phase Fraction of a (Ø50×200 mm) Sample of 45 Steel During Cooling Time Without Reinforcement.

While the alloy reached the liquidus temperature (T_l) at ¼ of the casting's diameter for the same sample after 23.8 seconds, the solidus temperature (T_s) was reached after 119.5 seconds. At the sample's center, the alloy reached T_l after 32.8 seconds (Figures 6-7) and T_s after 232.0 seconds, at which point the liquid phase disappears across all sections of the casting.

A Sample with a Diameter of 50 mm and 50% Reinforcement:

During the simulation of the cooling process of a 50 mm diameter sample of medium-carbon steel (grade 45) in a mold using reinforcement phase (MRP), occupying half of the sample's radius, it was observed that at the metal-mold contact surface, the alloy reached the liquidus temperature (T_l) after 3.4 seconds (Figure 8) and the solidus temperature (T_s) after 52.9 seconds.

In the same period, at a point equivalent to ¼ of the casting's diameter and at the metal-MRP boundary, the alloy reached T_l after 4.7 seconds (Figure 8) and T_s after 68.0 seconds. At the interface between the melt and the MRP near the center, the alloy reached T_l after 1.8 seconds (Figure 8) and T_s after 82.0 seconds, at which point the liquid phase disappeared entirely across all sections of the casting, as shown in Figure 9.

http://www.doi.org/10.62341/jfaa2057

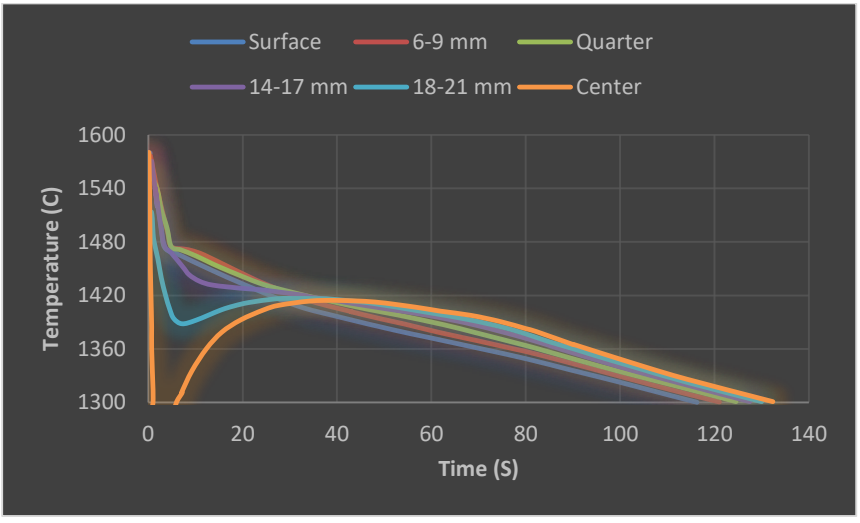

Figure 8 – Solidification and Cooling Kinetics of the Casting (Diameter 50 × 200 mm) Made of 45 Steel with 50% Reinforcement.

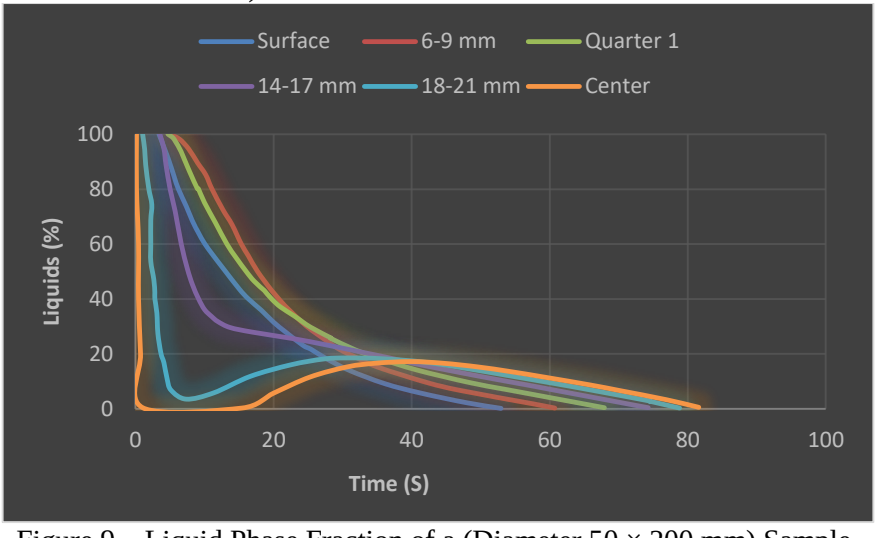

Figure 9 – Liquid Phase Fraction of a (Diameter 50 × 200 mm) Sample of 45 Steel with 50% Reinforcement.

It is worth noting that under these conditions, the temperature at the interface where the melt contacts the reinforcement particles (MRP) rises to a maximum of 1410°C within 5 seconds, then cools at a rate of 1.5–2.0°C/second, as shown in Figure 10.

http://www.doi.org/10.62341/jfaa2057

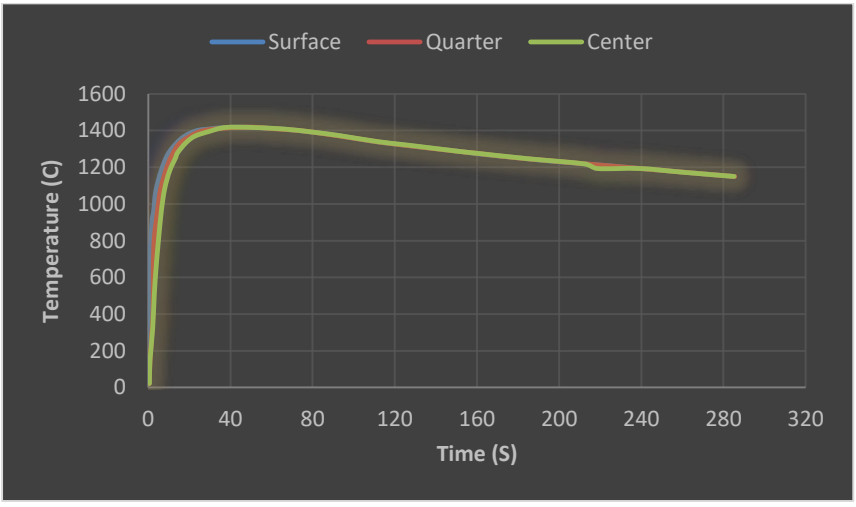

Figure 10 – Heating and Cooling Kinetics of the Reinforcement Phase (MRP).

It is also important to note that the rate of heat removal from the melt until the liquidus temperature (T_l) is reached varies across all experiments. When the sample solidifies in a mold without MRP, this rate ranges from 70–260°C/second, with the lower value corresponding to the central part of the sample, while the final cooling rate is 6.5-8.5°C/second, with the higher value corresponding to the center of the sample. When the sample solidifies in a mold containing a reinforcement phase (MRP) representing 20%, the rate at which the melt reaches T_l ranges from 325–640°C/second, with the higher value corresponding to the region near the boundary of the reinforcement phase. The final cooling rate is 21.0–25.0°C/second, with the higher value corresponding to the contact surface between the metal and the reinforcement phase. For a sample solidified in a mold containing 50% reinforcement particles (MRP), the rate at which the melt reaches T_l ranges from 260–430°C/second, with the higher value corresponding to the region near the reinforcement phase boundary. The final cooling rate is 19–21°C/second, with the higher value corresponding to the contact surface between the metal and the reinforcement phase .Figure 11 shows the cooling rates for reinforcement ratios of 0%, 10%, 20%, 25%, 30%, 35%, 40%, and 50%.

http://www.doi.org/10.62341/jfaa2057

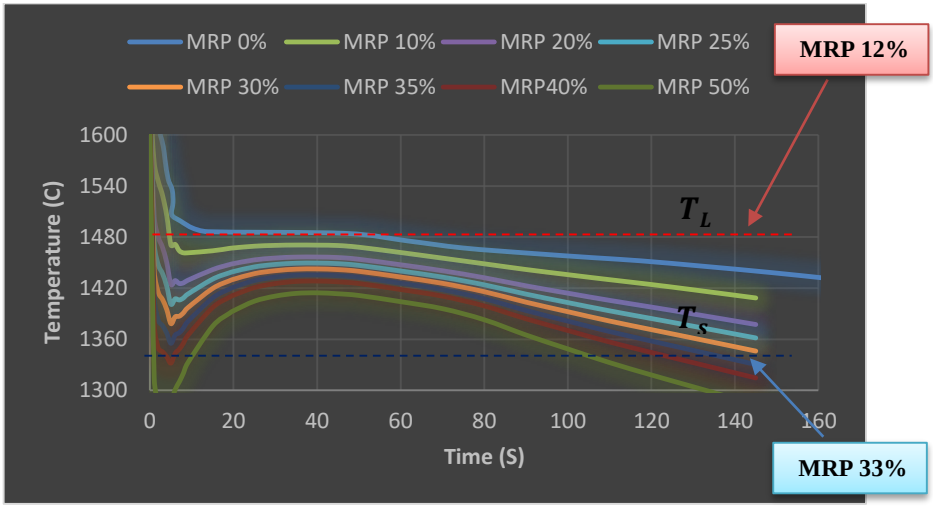

Figure 11 – Cooling Rates for Different Reinforcement Ratios.

Excessive reinforcement can cause the alloy to solidify before completing the casting process, as shown in Figure 11 for reinforcement curves of 50%, 40%, and 35%. This reduces the fluidity necessary to fill all mold cavities. Conversely, insufficient reinforcement can extend the solidification time, as seen in Figure 11 for reinforcement curves of 0% and 10%. This results in limited cooling rates, affecting grain size, solidification rates, and causing increased variation in microstructure across the sample. These factors may increase the likelihood of defects and residual internal stresses, ultimately impacting the mechanical properties of the casting compared to castings with optimal reinforcement.

Conclusion

The study demonstrated that integrating a metallic reinforcement phase (MRP) into medium-carbon 45 steel using casting with gasified patterns improves mechanical properties by accelerating cooling rates and enhancing the crystalline structure.

Computational simulations, mathematical calculations, and statistical analyses revealed significant variations based on reinforcement ratios. The optimal reinforcement ratio was found to range between 12% and 33%, depending on the shape, thickness, and design of the mold, as well as the distribution of reinforcement particles. This range ensures a balance between cooling rates and structural integrity while maintaining fluidity during casting.

http://www.doi.org/10.62341/jfaa2057

Reinforcement ratios exceeding 33% negatively impacted fluidity during pouring, highlighting the importance of precise reinforcement proportioning.

It is noteworthy that the presence of the reinforcement phase (MRP) in polystyrene patterns does not increase the quantitative indicators of harmful emissions. Instead, it reduces harmful emissions during casting and solidification by lowering cooling rates.

The study emphasizes the importance of adopting innovative mold designs that strategically integrate the reinforcement phase to achieve the desired performance while minimizing environmental emissions from casting processes.

These findings contribute to a deeper understanding of sustainable casting applications, offering insights into achieving a balance between mechanical performance and environmental considerations in industrial production processes. The study provides a solid foundation for exploring effective and eco-friendly casting techniques applicable across various industrial sectors.

References

[1] Balandyn G., 1979.: Bases of the casting theory formation. :// Machine building P.1, 328, & p.2. (in Russian)

[2] Cybrik A., 1977.: Physico-chemical processes in contact zone metal-mould. - K.- Science mind, – 211. (in Russian)

[3] Dulska, A., Studnicki, A. & Szajnar, J. (2017). Reinforcing cast iron with composite insert. Archives of Metallurgy and Materials. 62 (1), 355-357. DOI: 10.1515/amm-2017-0055 [in English].

[4] Gu, D., Chen, W., & Pan, Z. (2018). Laser additive manufactured WC reinforced Fe-based composites with gradient reinforcement/matrix interface and enhanced performance. Composite Structures. https://doi.org/xxxx

[5] Kang, N., Zhu, J., Chen, X., & Zhang, S. (2018). Selective laser melting of tungsten carbide reinforced maraging steel composite. Additive Manufacturing. https://doi.org/xxxx

[6] Tjong, S. C., & Lau, K. C. (1999). Sliding wear of stainless steel matrix composite reinforced with TiB2 particles. Materials Letters, 40(1), 61–67. https://doi.org/xxxx

[7] Oke, S. R., Obadele, B. A., Durowoju, M. O., & Adebayo, I. A. (2018). Influence of sintering process parameters on corrosion and wear behaviour of SAF 2205 reinforced with nano-sized

http://www.doi.org/10.62341/jfaa2057

TiN. Materials Chemistry and Physics, 216, 116–125. https://doi.org/xxxx

[8] Huang, Y., Li, D., Liu, X., & Ma, A. (2018). Microstructure and mechanical properties of 5083Al/Ti composites via submerged friction stir processing. Materials Science and Engineering: A, 732, 107-115.

[9] Rashad, M., Pan, F., Asif, M., She, J., & Ullah, M. (2015). Enhanced mechanical properties of Mg-Ti composites processed by powder metallurgy. Journal of Alloys and Compounds, 643, 61-69.

[10] Alaneme, K. K., Bodunrin, M. O., & Awe, O. (2018). Microstructural and mechanical properties of Al-Mg-Si alloy composites reinforced with steel particles. Materials Research Express, 5(3), 036501.

[11] Musbah J., Shalevska I., Obtaining Castings with Enhanced Structure Through Reinforcing Mold Patterns and Their Interaction During Pouring with the Liquid Phase, International Journal of Science and Technology, July 2021, Issue 26. .(inArabic)

[12] Shalevska, I. A. (2019). Issledovanie teploobmennyh processov v litejnoj forme s armirujushhej fazoj [Investigation of heat transfer processes in a mold with a reinforcing phase]. *Lit'e i metallurgija – Casting and Metallurgy, 3,* 54–59. https://doi.org/10.21122/1683-6065-2019-3-54-59

[13] Doroshenko V., Chichkan I., 2008.: Gas regime controlling of mould made of LSHM under obtaining large castings by Lost-foam process// Metal & Casting of Ukraine. –K.- № 11-12. – 35 – 38. (in Russian)

[14] Mamyshev V., Shinsky O., Sokolovskaya L., 2008.: About heat-physical influence of ingot with mold and casting in the cast structure formation // Casting and Metallurgy. - № 3, (special edition). –M-. 307 -309. (in Russian)

[15] Mamyshev V., Shinsky O., Sokolovskaya L., 2010.: System analysis of crystallization process of crystallization of cast raw pieces of different weights and purpose // Casing processes. – K.- 2010. - № 1. - 20 - 24. (in Russian)

[16] Ryabicheva L., Tsirkin A., Usatyuk D., 2010: Warm deformation of copper porous powder billets. TEKA. Edition of Lublin University of technology. Vol. XB, Lublin. (in English)

[17] Shalevskaya I., 2015.: Reducing harmful influence of foundry production on environment by the mean of progressive

http://www.doi.org/10.62341/jfaa2057

technologies // Russian Foundryman. – M. – № 1 – 37-39. (in Russian)

[18] Shalevskaya I., Bogdan A., Shinsky V., 2015.: Ecological monitoring harmful wastes development in th Lost-foam foundry// Metal & Casting of Ukraine. — K. — № 2 —32-36. (in Russian).

[19] Abraham, A. A., Dinaharan, I., Selvam, D. R., & Akinlabi, E. T. (2019). Influence of vanadium particle reinforcement on the mechanical properties of AA6063 aluminum alloy composites. Journal of Materials Research and Technology, 8(3), 2476-2483.

[20] ESI Group. (2013). *ESI Talk Magazine – Issue 5*. Retrieved fromhttps://www.slideshare.net/slideshow/esi-talk-magazine/25448197

[21] ESI Group. (2021). *ESI ProCAST 2021.5 – Release Highlights*. https://www.esi-group.com/products/virtual-manufacturing/casting/procast

[22] Bhadeshia, H. K. D. H., & Honeycombe, R. W. K. (2017). Steels: Microstructure and Properties (4th ed.). Elsevier.

[23] ASM International. (1993). ASM Handbook, Volume 1: Properties and Selection: Irons, Steels, and High-Performance Alloys (10th ed.). Materials Park, OH: ASM Internationa.

[24] Kőrösy, G., Roósz, A., & Mende, T. (2024). The Concept of the Estimation of Phase Diagrams (An Optimised Set of Simplified Equations to Estimate Equilibrium Liquidus and Solidus Temperatures, Partition Ratios, and Liquidus Slopes for Quick Access to Equilibrium Data in Solidification Software) Part I: Binary Equilibrium Phase Diagrams. *Metals*, *14*(11), 1266. https://doi.org/10.3390/met14111266.

[25] Shinsky, I., Shalevska, I., Musbah, J. (2015). Efficiency of influence of a metal macroreinforcing phase on process of solidification of large-sized castings. TEKA. Edition of Lublin University of technology, 15 (2), 51–59.